Cancer Management and Research

Dovepress

open access to scientific and medical research

Open Access Full Text Article

ORIGINAL RESEARCH

CircSKA3 Modulates FOXM1 to Facilitate Cell Proliferation, Migration, and Invasion While Confine Apoptosis in Medulloblastoma via miR-383-5p

This article was published in the following Dove Press journal:
Cancer Management and Research

Xinfang Wang*
Dong Xu*
Xin Pei
Yingying Zhang
Yuling Zhang
Yaxing Gu
Ying Li

Department of Pediatrics, Shandong Provincial Western Hospital, Jinan 250022, Shandong, People's Republic of China

*These authors contributed equally to this work

Background: Medulloblastoma (MB) is the most common malignant brain tumor during childhood. Circular RNA (circSKA3) was identified to function as an oncogene in MB. However, the mechanism of circSKA3 in MB remains unclear.

Methods: The levels of circSKA3, microRNA-383-5p (miR-383-5p), and forkhead box M1 (*FOXM1*) in MB tissues were measured by quantitative real-time polymerase chain reaction (qRT-PCR). The cell viability and apoptotic rate were assessed via 3-(4,5-dimethyl-2-thiazolyl)-2,5-diphenyl-2-H-tetrazolium bromide (MTT) assay and flow cytometry, respectively. The protein levels of B-cell lymphoma 2 (Bcl-2), C-Caspase3, and FOXM1 were detected via Western blot assay. Cell cycle was detected by flow cytometry. The migration and invasion abilities were monitored by Transwell assay. The dual-luciferase reporter assay was constructed to verify the interactions between miR-383-5p and circSKA3 or *FOXM1*. The mice model experiment was carried out to validate the effects of circSKA3 in vivo.

Results: The levels of circSKA3 and *FOXM1* were significantly elevated, while the level of miR-383-5p was notably declined in MB tissues. CircSKA3 was validated to sponge miR-383-5p, and *FOXM1* was a candidate target of miR-383-5p. CircSKA3 silencing impeded cell proliferation, migration, and invasion while promoted apoptosis by targeting miR-383-5p in vitro and retarded xenograft tumor growth in vivo. miR-383-5p suppressed cell proliferation, migration, and invasion but promoted apoptosis in MB cells by regulating FOXM1. CircSKA3 depletion decreased *FOXM1* expression via miR-383-5p in MB cells.

Conclusion: CircSKA3 augmented MB progression partly through miR-383-5p/*FOXM1* axis.

Keywords: circSKA3, miR-383-5p, *FOXM1*, medulloblastoma

Introduction

Medulloblastoma (MB) is a malignant brain tumor in children,[1,2] with high heterogeneity and aggressive. MB consists of many different molecular subtypes. Based on the significant differences in genetics, demography, and clinical characteristics, MB was classified as four distinct molecular subtypes: WNT, SHH, Group 3, and Group 4.[3,4] Current treatment methods including surgery, radiotherapy, and chemotherapy have contributed to the overall survival rate of MB patients, which the overall survival rates reached 75%.[5,6] However, there is a high probability for MB survivors to suffer from long-term side effects, including neurological,

Correspondence: Ying Li
Department of Pediatrics, Shandong Provincial Western Hospital, No. 4 Duanxing West Road, Jinan, Shandong 250022, People's Republic of China
Tel +86-531 83086400
Email dedfedx@163.com

submit your manuscript | www.dovepress.com
DovePress
http://doi.org/10.2147/CMAR.S272753

neuroendocrine, and psychosocial deficits in the growing process of children.[7,8] Therefore, it is urgent to search for novel therapeutic targets for MB patients.

With the development of next-generation sequencing methods, the aberrant expression of non-coding RNAs (ncRNAs) and their crucial roles in tumor were disclosed.[9] Mounting research has suggested that ncRNAs are closely correlated with cancers including MB, through regulating gene transcription, translation, and epigenetic modification, and then affected multiple biological processes.[10–12] Circular RNAs (circRNAs) are a class of ncRNAs with a closed continuous loop without 5′ caps and 3′ tails.[13] The role of circRNAs has been extensively studied in various diseases. In recent years, the rapid evolution of high-throughput sequencing technique and bioinformatics helped us to realize that circRNAs was aberrantly expressed in mammalian cells and even higher than the linear RNA isoforms of its host genes.[14] The dysregulated circRNAs were observed in various cancers including bladder carcinoma, colorectal cancer, ovarian cancer, as well as MB.[15–17] CircSKA3 (hsa_circ_0029696) was derived from the host gene Spindle And Kinetochore Associated Complex Subunit 3 (SKA3). A recent research exhibited that circSKA3 was upregulated in breast cancer tumors and cells, and its ectopic expression promoted tumor progression by complexing with Tks5 and integrin β1.[18] Besides, research also showed that circSKA3 was highly expressed in MB, and circ-SKA3 could regulate cell proliferation, migration, and invasion in MB.[17] This suggested that circ-SKA3 exerted pivotal oncogenic role in the evolution and progression of MB. However, the underlying mechanisms of circSKA3 in MB were unknown.

It is generally accepted that circRNAs functioned as "sponges" of miRNAs and participated in post-transcriptional regulation, and further reduced their ability to target mRNAs.[19] MiRNAs are a form of small RNAs (~22 nts) with no translation ability and mediate the messenger RNA (mRNA) expression or stability.[20] Sufficient evidence showed that miRNAs were aberrantly expressed in MB.[21,22] MiR-383-5p, a tumor suppressor, was reported to be downregulated in many human cancers including ovarian cancer,[23] cervical cancer,[24] and gastric carcinoma.[25] However, no studies have yet disclosed its role in MB.

Forkhead box M1 (*FOXM1*), a member of the Forkhead family of transcription factors, could bind to DNA sequence in the enhancer region of various target genes.[26] *FOXM1* was found to be involved in the development of many different types of tumor such as hepatocellular carcinoma[27] and renal cell carcinoma.[28] The pivotal role of *FOXM1* in MB has been widely studied. *FOXM1* was highly expressed in all subtypes of MB, and its expression level was significantly correlated with the unfavorable clinical outcome of MB, which indicated that *FOXM1* could be used as an additional prognostic marker and a potential novel target for MB treatment.[29] Besides, knockdown of FOXM1 expression could inhibit cell proliferation and invasion, and induce apoptosis by caspase 3/7 pathway.[30] However, the effect of FOXM1 in MB needs to be further illuminated.

In this research, we aimed to explore the underlying mechanism of circSKA3 in MB, and this may provide a novel therapeutic target for MB patients.

Materials and Methods

Tissue Samples Collection

The study was permitted by the Ethics Committee of Shandong Provincial Western Hospital and executed according to the Declaration of Helsinki Principles (IRB No.2019SD662). Twenty tissue samples and corresponding adjacent normal tissue samples were obtained from Shandong Provincial Western Hospital. The clinicopathological features of subjects are exhibited in Table 1. All tissues were frozen at −80°C until further used. Written informed consents were obtained from the adult patients, or from the parents or legal guardians of the child patients.

Table 1 The Clinicopathological Features of Medulloblastoma Patients

Clinicopathological Features	Number of Cases
Age(years)	
>3	12
≤3	8
Gender	
Male	14
Female	6
Histological subtype	
Classic	15
Desmoplastic	4
Large cell/anaplastic	1
Metastasis at diagnosis	
Absence	18
Presence	2

Quantitative Real-Time Polymerase Chain Reaction (qRT-PCR)

The RNA in MB tissues or cells was extracted using TriQuick Reagent (Solarbio, Beijing, China). The reverse transcription was performed using a transcription kit (Solarbio), and the quantitative PCR was carried out using SYBR Premix Ex Taq II (TaKaRa, Dalian, China) on a 96-well Real-Time PCR Detection System (Bio-Rad, Shanghai, China). The levels of circSKA3, *FOXM1,* and miR-383-5p were normalized by glyceraldehyde 3-phosphate dehydrogenase (*GAPDH*) or small nuclear RNA *U6*, and then calculated by the $2^{-\Delta\Delta Ct}$ method. The oligonucleotides of primers were obtained from Beijing Genomics Institute (BGI, Shenzhen, China) and exhibited as follows: circSKA3: (F, 5′-TGGGACTTCTGTACCATAAAGCAT-3′, and R, 5′-ATCTATGGCCTCCTCACTGGT-3′); miR-383-5p: (F, 5′-CGCGCGCAGATCAGAAGGTGA-3′, and R, 5′-ATCCAGTGCAGGGTCCGAGG-3′); *FOXM1*: (F, 5′-ATGGCAAATTTTTCGCTCC-3′, and R, 5′-ATG TCACCAGAAATTCCCAGTT-3′); *GAPDH*: (F, 5′-TGT TCGTCATGGGTGTGAAC-3′, and R, 5′-ATG GCATGGACTGTGGTCAT-3′), and *U6*: (F, 5′-ATT GGAACGATACAGAGAAGATT-3′, and R, 5′-GGA ACGCTTCACGAATTTG-3′).

Cell Culture and Transfection

Two medulloblastoma cell lines DAOY and ONS-76 were purchased from Shanghai YaJi Biological (Shanghai, China). The cells were cultivated in Dulbecco's modified Eagle's medium (DMEM; Solarbio) containing 10% fetal bovine serum (FBS; Solarbio) and 1% penicillin/streptomycin (Solarbio) in a 5% CO_2 incubator at 37°C.

Small interfering RNA (siRNA) against circSKA3 (si-circSKA3, final concentration, 20 nM) and matched negative control (si-NC, final concentration, 20 nM), miR-383-5p mimic (miR-383-5p, final concentration, 10 nM) and negative control (miR-NC, final concentration, 10 nM), miR-383-5p inhibitor (anti-miR-383-5p, final concentration, 25 nM) and its scramble (anti-miR-NC, final concentration, 25 nM), siRNA targeting FOXM1 (si-*FOXM1*, final concentration, 20 nM) and its control (si-NC, final concentration, 20 nM) were synthesized in GenePharma (Shanghai, China). The fragments of *FOXM1* were inserted into pcDNA3.1 (vector; Invitrogen, Carlsbad, CA, USA) to construct overexpression plasmid (FOXM1, final concentration, 1 μg/mL). Cell transfection was carried out using Lipofectamine 2000 (Invitrogen) according to the manufacturer's instructions. In brief, 4×10^5 DAOY and ONS-76 cells were cultured for 24 h to grow to subconfluence, the miRNA mimic or inhibitor, siRNA, and plasmids were transfected into the cells. Twenty-four or 48 hours upon transfection, the cells were harvested for further research.

RNase R Digestion

Total RNA in MB cells was extracted using TriQuick Reagent (Solarbio, Beijing, China). Five micrograms of total RNA were incubated with RNase R (Epicenter Biotechnologies, Shanghai, China) at a concentration of 3 U/μg. After total RNA incubation with RNase R for 15 min at 37°C, the expression of circSKA3 was examined using qRT-PCR.

Subcellular Localization

Cytoplasmic & Nuclear RNA Purification Kit (Norgen Biotek Corp., Belmont, MA, USA) was used to determine the localization of circSKA3. Cells were lysed by the Lysis Buffer J, and then cell lysates were centrifuged. Then, the nuclear RNA and cytoplasmic RNA were added into anhydrous ethanol and Buffer SK, respectively. Subsequently, the nuclear RNA and cytoplasmic RNA were eluted by the spin column. Finally, the proportion of circSKA3 in cytoplasmic and nucleus fractions was detected using qRT-PCR.

3-(4,5-Dimethyl-2-Thiazolyl)-2,5-Diphenyl-2-H-Tetrazolium Bromide (MTT) Assay

The cell viability of DAOY and ONS-76 cells was detected using MTT (Solarbio). The DAOY and ONS-76 cells (3×10^3 per well) were firstly injected into a 96-well plate and cultivated for 24 h. Following transfection, the cells were incubated for another 0 h, 24 h, 48 h, and 72 h. MTT was injected into each well and maintained for 4 h at 37°C. Then, dimethyl sulfoxide (DMSO) was added to dissolve the formazan for 10 min at 37°C. Then, the absorbance was tested on a microplate reader.

Flow Cytometry Analysis of Cell Apoptosis and Cell Cycle

The apoptotic rate of DAOY and ONS-76 cells was assessed using Annexin V-fluorescein isothiocyanate (FITC)/propidium iodide (PI) apoptosis detection kit (Solarbio, Beijing, China). The DAOY and ONS-76 cells were firstly re-suspended in binding buffer and then

incubated with Annexin V-FITC for 10 min in the dark. Then, the cell samples were incubated with PI for another 5 min in the dark. Within 1 h, the apoptotic rate of cell samples was evaluated on flow cytometry. For detection of cell cycle, cells were stained with PI for 30 min. Cell cycle distribution was detected by flow cytometry.

Western Blot Assay

Total protein in DAOY and ONS-76 cells was extracted using RIPA regent (Solarbio), and a protein assay kit (Beyotime, Shanghai, China) was utilized to measure the concentration of protein samples. Then, the protein samples (30 μg/lane) were separated by 12%-15% sodium dodecyl sulfonate-polyacrylamide gel electrophoresis (SDS-PAGE) and electrophoresed at 4°C for 1 h at a constant voltage of 70 V and another 1.5 h at a constant voltage of 110 V. Then, the blots were transferred onto a polyvinylidene fluoride (PVDF) membrane (GE Healthcare, Piscataway, NJ, USA). Subsequently, the membrane was blocked with 5% non-fat milk dissolved in TBST for 4 h at 37°C and incubated with primary antibodies: anti-B-cell lymphoma 2 (Bcl-2; ab32124, 1:1000; Abcam, Cambridge, MA, USA), C-Caspase3 (ab32042, 1:500; Abcam) or anti-GAPDH (ab8245, 1:10000; Abcam) overnight at 4°C. Then, the membrane was incubated with goat anti-rabbit secondary antibody (ab216773, 1:10000; Abcam) for another 3 h at 37°C. The primary antibodies were dissolved in 3% BSA with TBST, and the secondary antibody was dissolved in TBST. The intensity of bands was examined by an ECL kit (Beyotime).

Transwell Assay

The Transwell assay was conducted to detect the migrated and invaded abilities of DAOY and ONS-76 cells. For cell migration, the lower Transwell chamber (Corning, Tewksbury, MA, USA) was added with DMEM with 10% FBS, while the upper one was injected with DAOY and ONS-76 cells in DMEM without FBS. Following 24-h cultivation, the migrating cells on the backside of polycarbonate film were fixed with 4% methanol for 20 min and then stained with 0.1% violet crystal for 15 min. The cells in 10 randomly selected fields were counted under a microscope. Original magnification, 200×.

For cell invasion, the protocols were similar to cell migration. While the difference is the upper chamber was coated with Matrigel matrix (BD Biosciences, San Jose, CA, USA).

Dual-Luciferase Reporter Assay

The wild type (containing the complementary binding sites) and mutant fragments of circSKA3 or 3′-untranslated regions (3′UTR) of FOXM1 were cloned and inserted into pGL3 vector (Promega, Madison, WI, USA) to construct the dual-luciferase reporter, named as circSKA3 WT, circSKA3 MUT, *FOXM1* 3′UTR WT, or *FOXM1* 3′UTR MUT. The co-transfection of luciferase reporter and miR-NC or miR-383-5p was performed using Lipofectamine 2000 (Invitrogen). The luciferase activity was evaluated using Dual-Lucy Assay Kit (Solarbio).

Mice Xenograft Models

The nude mice experiment was performed according to the procedures approved by the Animal Care Committee of Shandong Provincial Western Hospital. Animal studies were performed in compliance with the ARRIVE guidelines and the Basel Declaration. All animals received humane care according to the National Institutes of Health (USA) guidelines. The DAOY cells (5×10^6) stably transfected with sh-NC or sh-circSKA3 were injected subcutaneously into the right flank of the six-week-old male nude mice (n=6 per group). Following injection, the xenograft tumor was measured every 7 days for 5 times and calculated according to the formula: volume (mm^3) = width^2 × length/2. At 35-d measurement, the xenograft tumors were resected from nude mice. The xenograft tumors' weight was measured, and the tumors were stored for the next exploration.

Statistical Analysis

GraphPad Prism 7 (GraphPad Inc., La Jolla, CA, USA) was used to perform the experiment data. All quantitative data were presented as the mean ± standard deviation (SD) of at least three biological replicates carried out at the same time. Sample size ("n") always represents biological replicates. The differences between the two groups were processed by Student's *t*-test, and the differences among multiple groups were evaluated by one-way analysis of variance (ANOVA). Statistical significance was defined as P value <0.05.

Results

CircSKA3 Was Significantly Increased in MB Tissues

In order to explore the role of circSKA3 in MB, the level of circSKA3was firstly measured in MB tissues. As presented in Figure 1A, the level of circSKA3 was dramatically up-regulated in MB tissues compared to that in adjacent normal tissues. Moreover, the results confirmed that circSKA3 was indeed circRNA, which was resistant to RNase R digestion (Figure 1B and C). Research has shown that circRNAs located

in the nucleus mainly regulate the transcription of the parental gene, while in the cytoplasm, circRNAs could be used as endogenous competitive RNAs (ceRNA), thereby regulating the physiological activities of tumor cells.[31] Subsequently, we measured the subcellular localization of circSKA3 by nuclear and cytoplasmic separation experiments. The result suggested that circSKA3 was mostly located in the cytoplasm of DAOY and ONS-76 cells (Figure 1D and E). These data indicated that circSKA3 was a circRNA and was upregulated in MB.

CircSKA3 Knockdown Suppressed Cell Proliferation, Migration, and Invasion but Induced Apoptosis in DAOY and ONS-76 Cells

To explore the functions of circSKA3 in MB, si-circSKA3 was transfected into DAOY and ONS-76 cells. As exhibited in Figure 2A and B, transfection of si-circSKA3 induced a near 50% reduction in circSKA3 expression in DAOY and ONS-76 cells in contrast with the si-NC group. The following MTT assay indicated that the transfection of si-circSKA3 in DAOY and ONS-76 cells resulted in a near 30% reduction of cell viability related to that in the si-NC group (Figure 2C and D). However, the apoptosis rate was increased by 15% in DAOY and ONS-76 cells transfected with si-circSKA3 (Figure 2E and F). Since Bcl-2 and C-Caspase3 as apoptosis-related markers, we detected levels of these proteins in si-circSKA3-transfected DAOY and ONS-76 cells. As showed in Figure 2G and H, the protein level of Bcl-2 was decreased by half, while the protein level of C-Caspase3 was 3–4 fold enhanced in DAOY and ONS-76 cells transfected with si-circSKA3. Moreover, the proportion of the S-phase cells was reduced, while the G1/G0-phase cells were increased after circSKA3 knockdown (Figure 2I and J). Besides, the number of migration and invasion cells was both reduced in DAOY and ONS-76 cells transfected with si-circSKA3 (Figure 2K and L). These results demonstrated that the depletion of circSKA3 blocked MB progression in vitro.

MiR-383-5p Was Negatively Interacted with circSKA3 in DAOY and ONS-76 Cells

As shown in Figure 3A and B, circSKA3 was enriched by circSKA3 probe in both DAOY and ONS-76 cells. To investigate the biological mechanism of circSKA3 in MB, starBase was used to search the putative targets of circSKA3. Venn diagram showed that miR-382-5p, miR-383-5p, miR-520g-3p, miR-520h, and miR-576-5p harbored the binding sites of circSKA3 (Figure 3C). Moreover, miR-

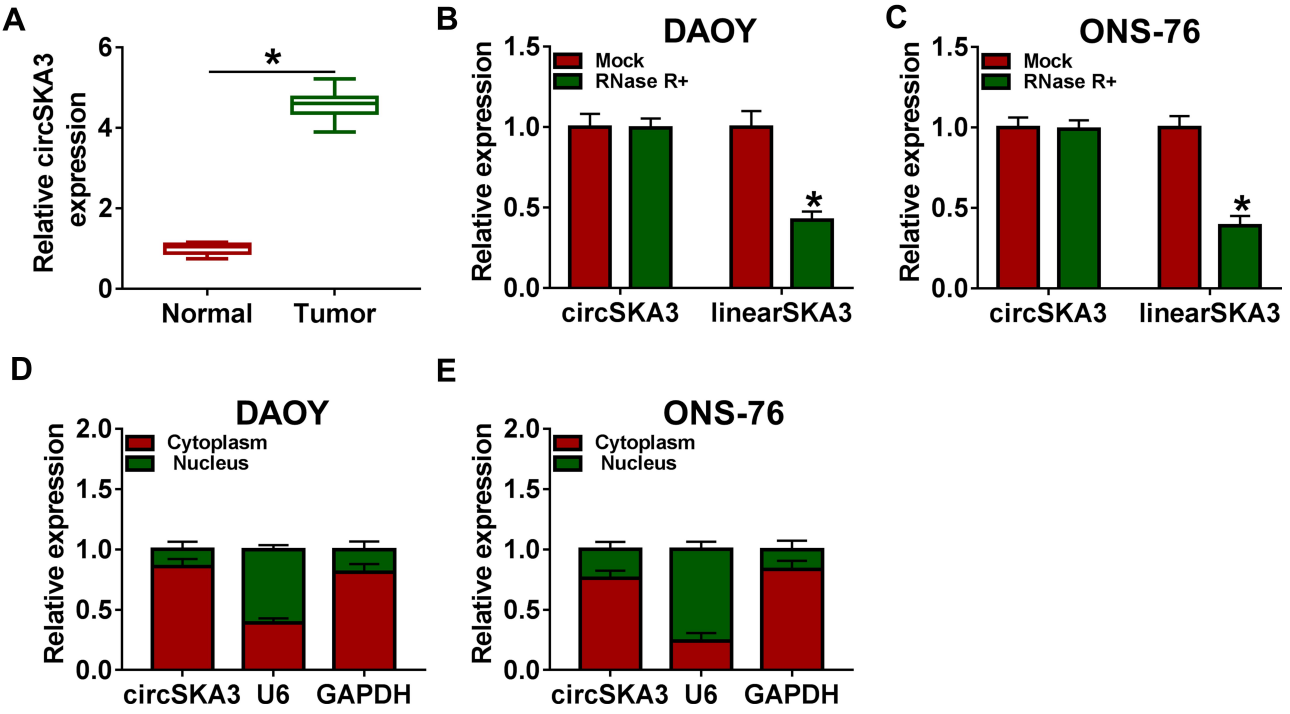

Figure 1 CircSKA3 was significantly increased in MB tissues. (**A**) The level of circSKA3 in 20 MB tissues and adjacent normal tissues was tested by qRT-PCR. (**B** and **C**) CircSKA3 resistance to RNase R was detected by qRT-PCR. (**D** and **E**) QRT-PCR was used to assess the level of cytoplasmic control transcript (*GAPDH*), nuclear control transcript (*U6*) and circSKA3 in nuclear and cytoplasmic fractions. Error bar, SD; n=3 biological replicates. *P<0.05.

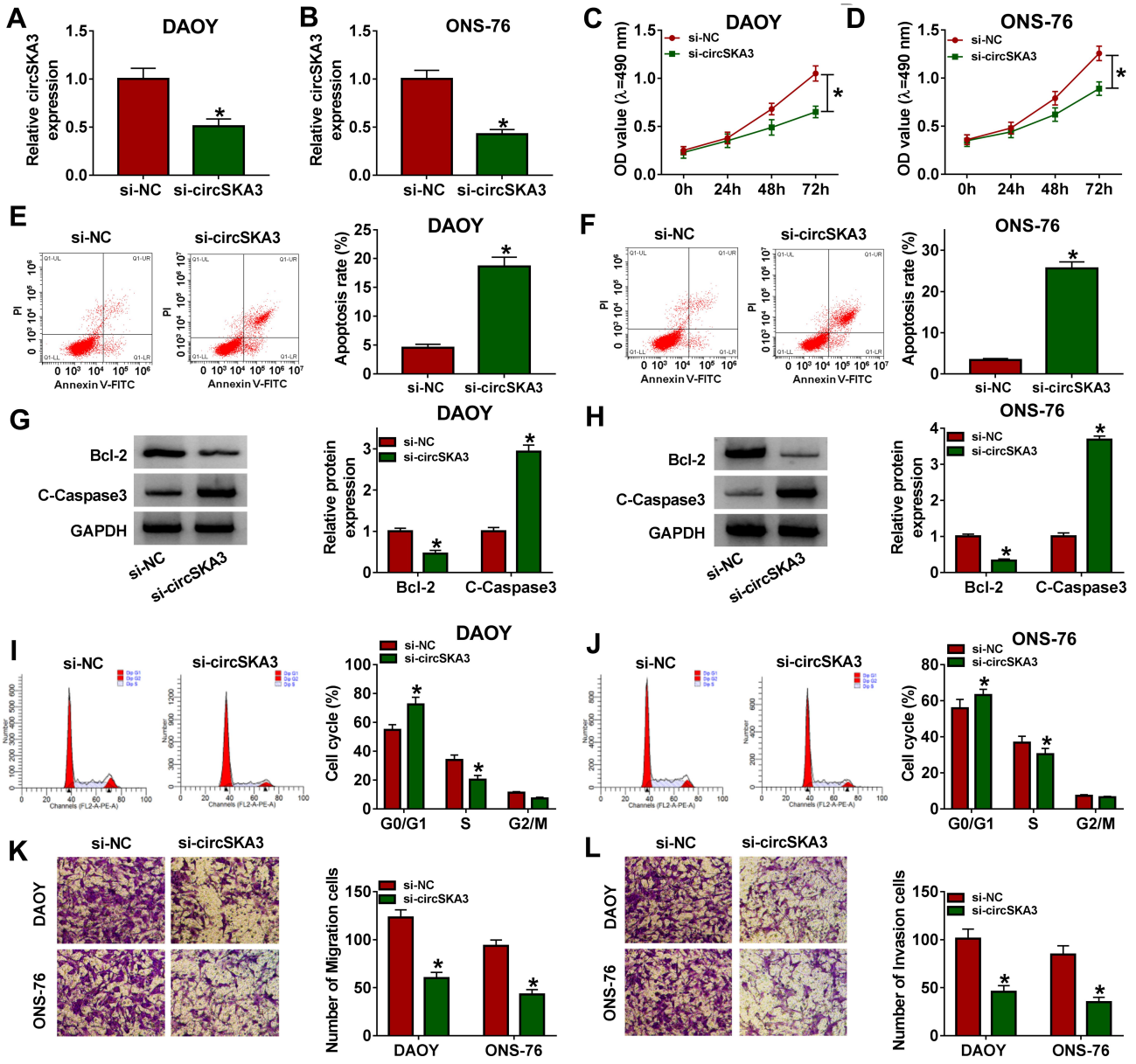

Figure 2 CircSKA3 knockdown suppressed cell proliferation, migration, and invasion but induced cell apoptosis and cycle arrest in DAOY and ONS-76 cells. (**A**–**L**) The DAOY and ONS-76 cells were transfected with si-NC or si-circSKA3. (**A** and **B**) The level of circSKA3 was tested by qRT-PCR. (**C** and **D**) The cell viability was examined via MTT assay. (**E** and **F**) The apoptotic rate was measured through flow cytometry. (**G** and **H**) The protein levels of Bcl-2 and C-Caspase3 were assessed by Western blot assay. (**I** and **J**) Cell cycle distribution was determined by flow cytometry. (**K** and **L**) The migration and invasion abilities were detected by Transwell assay. Error bar, SD; n=3 biological replicates. *P<0.05.

382-5p, miR-383-5p, miR-520g-3p, miR-520h, and miR-576-5p were captured by circSKA3 probe, and then the enrichment of miRNAs was detected by qRT-PCR. As shown in Figure 3D and E, miR-383-5p exhibited the highest expression, which indicated that circSKA3 exhibited the strongest interaction with miR-383-5p. Thus, miR-383-5p was selected for further research. As presented in Figure 3F, miR-383-5p had complementary biding sites with circSKA3. Following dual-luciferase reporter assay implied that the transfection of miR-383-5p contributed to the notable decline of luciferase activity of circSKA3 WT reporter in contrast to that in the miR-NC group, while the luciferase activity of circSKA3 MUT reporter had no change in any group (Figure 3G and H). In addition, the level of miR-383-5p was obviously increased in si-circSKA3-transfected DAOY and ONS-76 cells (Figure 3I). Besides, the data indicated that miR-383-5p was significantly decreased in MB tissues (Figure 3J). These data disclosed that miR-383-5p was decreased in DAOY and ONS-76 cells and was a target of circSKA3 in MB tissues.

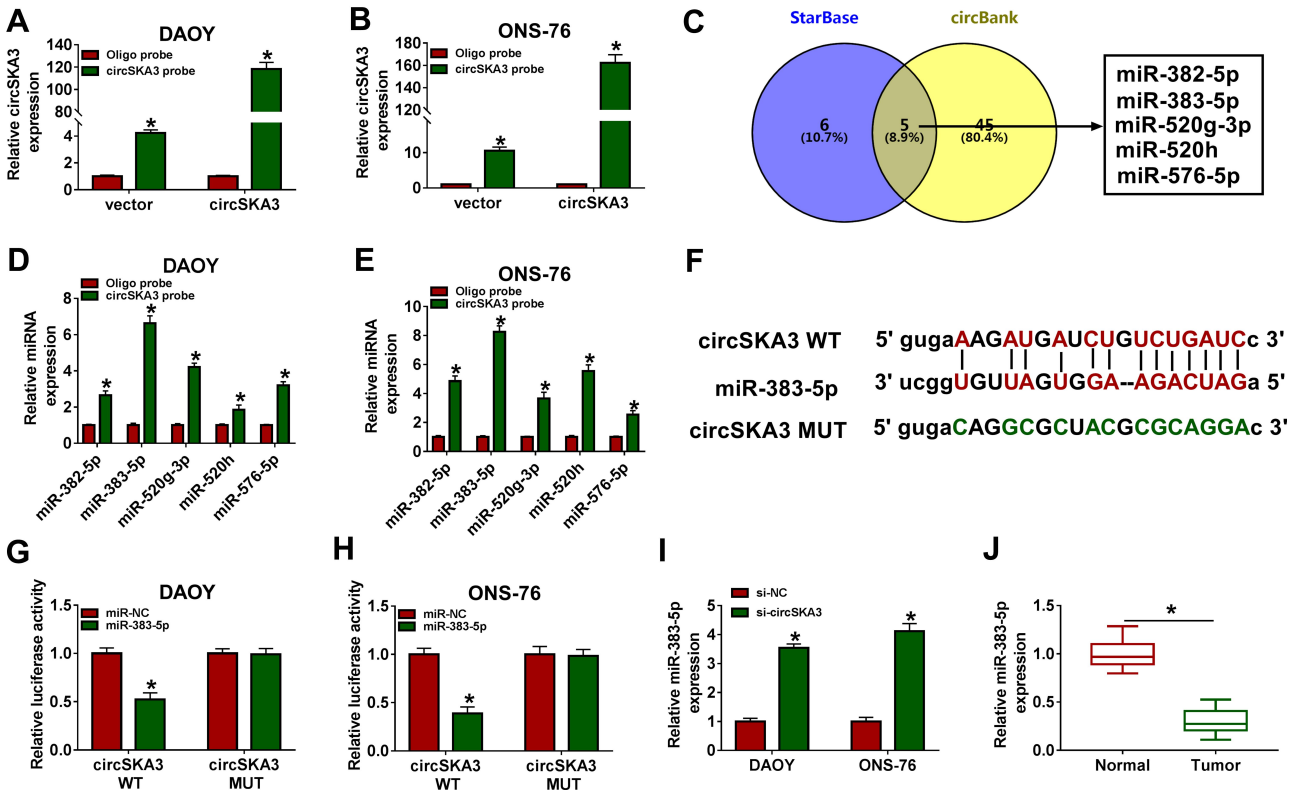

Figure 3 miR-383-5p was negatively interacted with circSKA3 in DAOY and ONS-76 cells. (**A** and **B**) The expression of circSKA3 was detected by qRT-PCR. (**C**) Venn diagram showed that miR-382-5p, miR-383-5p, miR-520g-3p, miR-520h and miR-576-5p contained the binding sites of circSKA3. (**D** and **E**) The enrichment of miR-382-5p, miR-383-5p, miR-520g-3p, miR-520h and miR-576-5p was detected RNA pull down assay using circSKA3 probe. (**F**) The complementary binding sites between miR-383-5p and circSKA3 were displayed, as well as the mutant sequences of circSKA3. (**G** and **H**) The luciferase activity of circSKA3 WT or circSKA3 MUT reporter in DAOY and ONS-76 cells transfected with miR-NC or miR-383-5p was detected via dual-luciferase reporter assay. (**I**) The level of miR-383-5p in DAOY and ONS-76 cells transfected with si-NC or si-circSKA3 was tested by qRT-PCR. (**J**) The level of miR-383-5p in 20 MB tissues and adjacent normal tissues was tested by qRT-PCR. Error bar, SD; n=3 biological replicates. *P<0.05.

CircSKA3 Facilitated Cell Proliferation, Migration, and Invasion While Repressed Apoptosis in DAOY and ONS-76 Cells by Regulating miR-383-5p

To explore the functions of circSKA3 and miR-383-5p in MB, anti-miR-383-5p and si-circSKA3 were co-transfected into DAOY and ONS-76 cells. As exhibited in Figure 4A and B, the level of miR-383-5p was evidently up-regulated in DAOY and ONS-76 cells transfected with si-circSKA3, while the introduction of miR-383-5p inhibitor mitigated the promotion effect on miR-383-5p. The absence of miR-383-5p relieved the cell viability in DAOY and ONS-76 cells inhibited by circSKA3 knockdown (Figure 4C and D). While the apoptotic rate was notably elevated in DAOY and ONS-76 cells transfected with si-circSKA3, but the transfection of miR-383-5p inhibitor attenuated this promotion effect (Figure 4E and F). Furthermore, miR-383-5p inhibitor weakened the inhibitory impact on the protein level of Bcl-2, as well as the accelerated impact on the protein level of C-Caspase3 in DAOY and ONS-76 cells caused by circSKA3 deletion (Figure 4G and H). Moreover, circSKA3 knockdown-induced promotion effect on G1/G0-phase cells and inhibition effect on S-phase cells were partially reversed by miR-383-5p inhibitor (Figure 4I and J). Besides, the migrated and invaded abilities were apparently declined in DAOY and ONS-76 cells transfected with si-circSKA3, while partly regained by the re-introduction of anti-miR-383-5p (Figure 4K and L). These data uncovered that circSKA3 accelerated MB progression in DAOY and ONS-76 cells by targeting miR-383-5p.

FOXM1 Was a Direct Target of miR-383-5p in DAOY and ONS-76 Cells

To illustrate the mechanism of miR-383-5p in MB, TargetScan was utilized to predict the potential targets of miR-383-5p. As presented in Figure 5A, the 3′UTR of *FOXM1* had complementary sequences with miR-383-5p. The luciferase activity of *FOXM1* 3′UTR WT reporter was significantly decreased in DAOY and ONS-

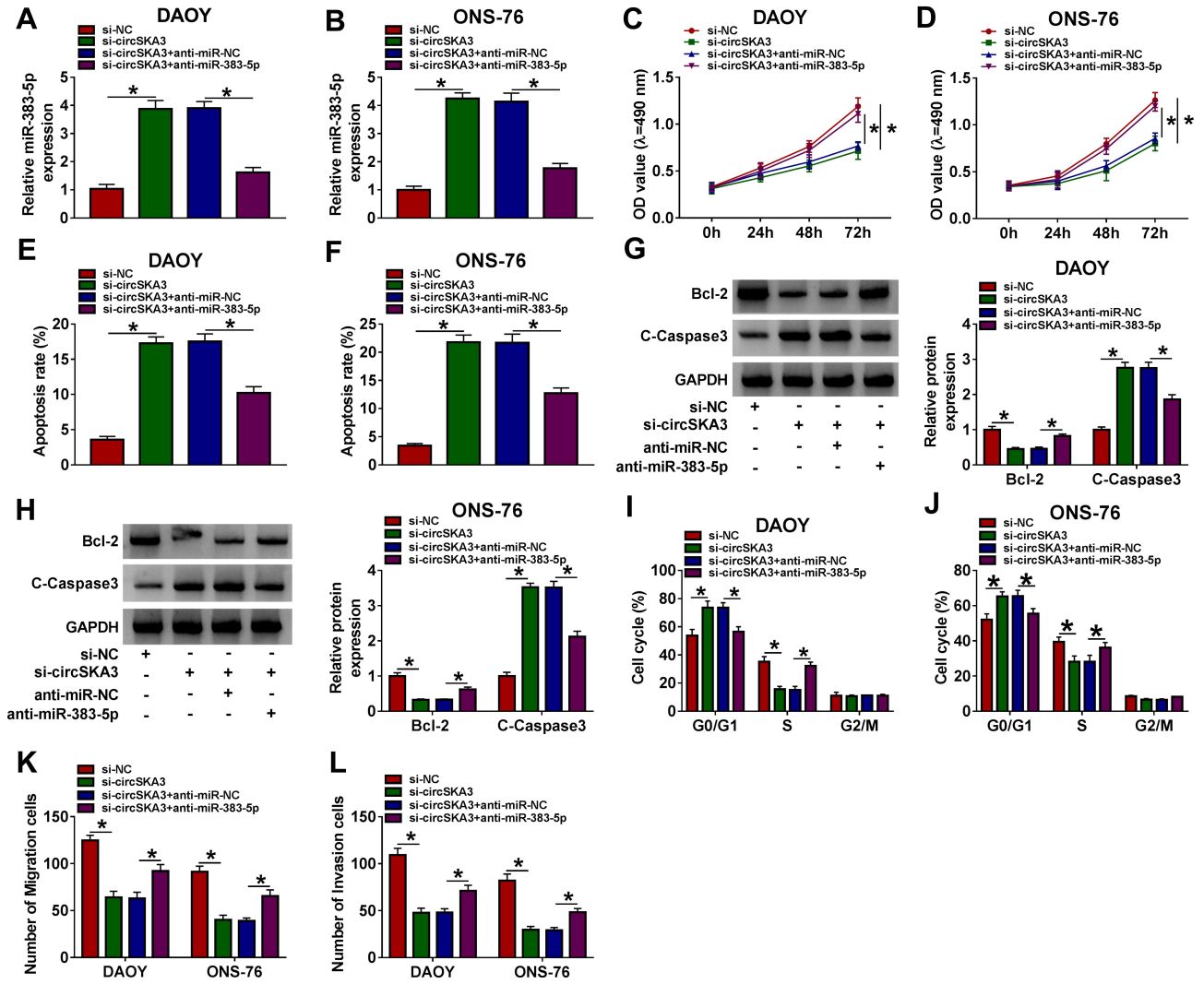

Figure 4 CircSKA3 facilitated cell proliferation, migration, and invasion while repressed apoptosis in DAOY and ONS-76 cells by regulating miR-383-5p. (**A**–**L**) The DAOY and ONS-76 cells were transfected with si-NC, si-circSKA3, si-circSKA3 + anti-miR-NC, si-circSKA3 + anti-miR-383-5p. (**A** and **B**) The level of miR-383-5p was examined by qRT-PCR. (**C** and **D**) The cell viability was monitored via MTT assay. (**E** and **F**) The apoptotic rate was assessed through flow cytometry. (**G** and **H**) The protein levels of Bcl-2 and C-Caspase3 were evaluated by Western blot assay. (**I** and **J**) Cell cycle arrest was measured by flow cytometry. (**K** and **L**) The migration and invasion abilities were tested by Transwell assay. Error bar, SD; n=3 biological replicates. *P<0.05.

76 cells transfected with miR-383-5p, while the luciferase activity *FOXM1* 3′UTR MUT reporter had no apparent fluctuation in any group (Figure 5B and C). Moreover, the protein expression of FOXM1 was suppressed by miR-383-5p in DAOY and ONS-76 cells (Figure 5D). The protein level of FOXM1 was remarkably reduced in DAOY and ONS-76 cells transfected with si-circSKA3, but partially regained in DAOY and ONS-76 cells co-transfected with si-circSKA3 and anti-miR-383-5p (Figure 5E). Besides, the mRNA and protein levels of FOXM1 were both conspicuously enhanced in MB tissues (Figure 5F and G). Taken together, *FOXM1* negatively interacted with miR-383-5p in DAOY and ONS-76 cells.

MiR-383-5p Confined Cell Proliferation, Migration, and Invasion While Facilitated Apoptosis in DAOY and ONS-76 Cells by Targeting *FOXM1*

To further explore the functions of miR-383-5p and *FOXM1* in MB, miR-383-5p and FOXM1 were co-transfected into DAOY and ONS-76 cells. As displayed in Figure 6A and B, the protein level of FOXM1 was notably declined in miR-383-5p-transfected DAOY and ONS-76 cells, while recovered in DAOY and ONS-76 cells co-transfected with miR-383-5p and FOXM1. The MTT assay and Transwell assay results indicated that the transfection of *FOXM1* overexpression rescued the cell viability, migrated, and invaded abilities

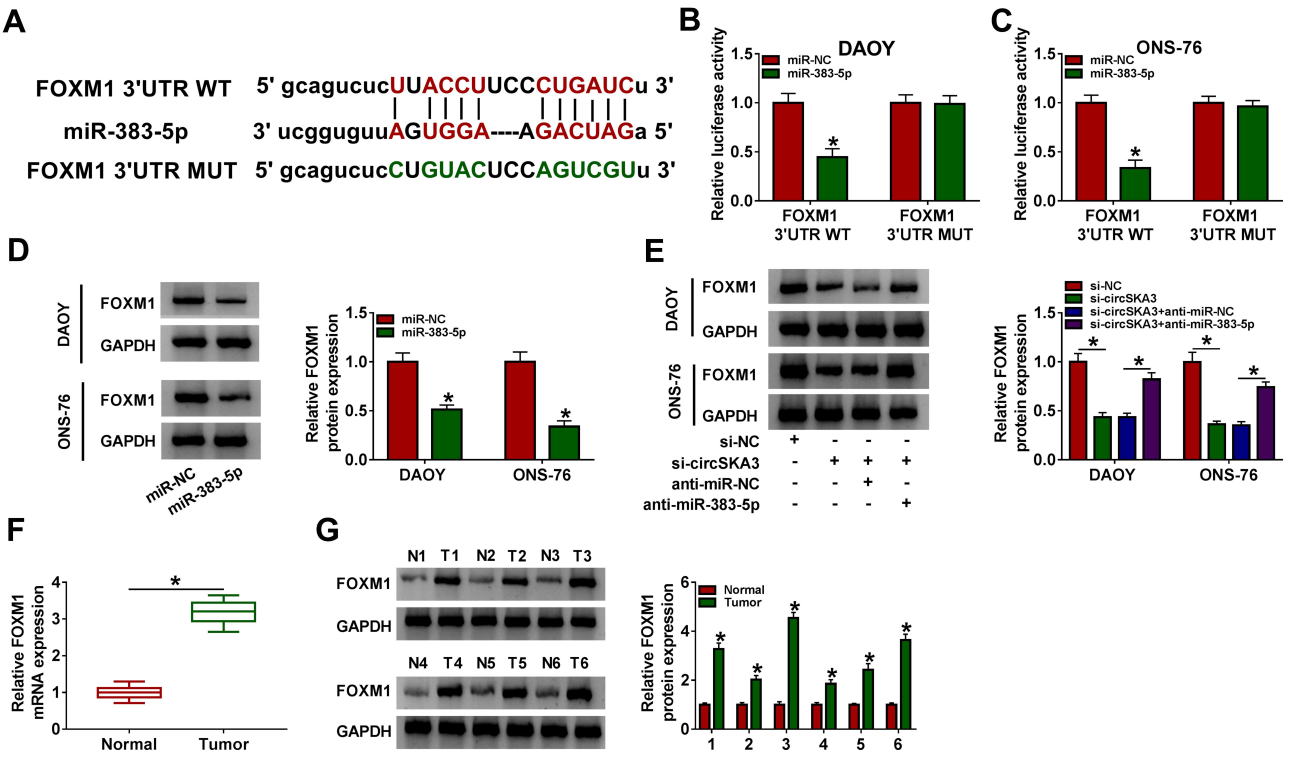

Figure 5 *FOXM1* was a direct target of miR-383-5p in DAOY and ONS-76 cells. (**A**) The complementary binding sites between miR-383-5p and *FOXM1* were exhibited, as well as the mutant sequences of *FOXM1*. (**B** and **C**) The luciferase activity of *FOXM1* 3′UTR WT or *FOXM1* 3′UTR MUT reporter in DAOY and ONS-76 cells transfected with miR-NC or miR-383-5p was detected via dual-luciferase reporter assay. (**D**) The protein level of FOXM1 in DAOY and ONS-76 cells transfected with miR-NC or miR-383-5p was tested by Western blot assay. (**E**) The protein level of FOXM1 in DAOY and ONS-76 cells transfected with si-NC, si-circSKA3, si-circSKA3 + anti-miR-NC or si-circSKA3 + anti-miR-383-5p was determined by Western blot. (**F**) The mRNA level of *FOXM1* was detected via qRT-PCR. (**G**) The protein level of FOXM1 was assessed by Western blot assay. Error bar, SD; n=3 biological replicates. **P*<0.05.

in DAOY and ONS-76 cells constrained by miR-383-5p (Figure 6C and D and K and L). However, the apoptotic rate and cell cycle showed the opposite trends. Briefly, the apoptotic rate was distinctly increased in the miR-383-5p group, while partially receded in miR-383-5p + FOXM1 group (Figure 6E and F). Furthermore, the introduction of FOXM1 upregulation counteracted the restraint effect on the protein level of Bcl-2 and the promoted effect on the protein level of C-Caspase3 in DAOY and ONS-76 cells caused by miR-383-5p overexpression (Figure 6G and H). Besides, miR-383-5p overexpression-induced cell cycle arrest was abolished by FOXM1 overexpression (Figure 6I and J). To sum up, miR-383-5p suppressed MB progression by regulating *FOXM1*.

CircSKA3 Silencing Confined Xenograft Tumor Growth in vivo

To further validate the effects of circSKA3 in MB, the mice model experiment was carried out. As presented in Figure 7A and B, the volume and weight of xenograft tumor were both markedly reduced in the sh-circSKA3 group in comparison with that in the sh-NC group. The level of circSKA3 was obviously down-regulated, but miR-383-5p was notably enhanced in the sh-circSKA3 group (Figure 7C and D). In addition, the protein level of FOXM1 was strikingly decreased in the sh-circSKA3 group (Figure 7E). These data unraveled that circSKA3 knockdown blocked xenograft tumor growth in vivo.

Discussion

Tumor progression is a complicated process in the human body. CircSKA3 was reported to implicate in tumor progression in MB. This research aimed to investigate the mechanism and functions of circSKA3 in MB. Our research demonstrated that circSKA3 knockdown restrained MB progression partially through miR-383-5p/*FOXM1* axis.

The ectopic expression of circSKA3 was associated with tumor progression. For example, Du et al reported that circSKA3 was dramatically increased in breast cancer, and its silencing constrained the invasive capacity of breast cancer cells in vitro and in vivo by binding integrin

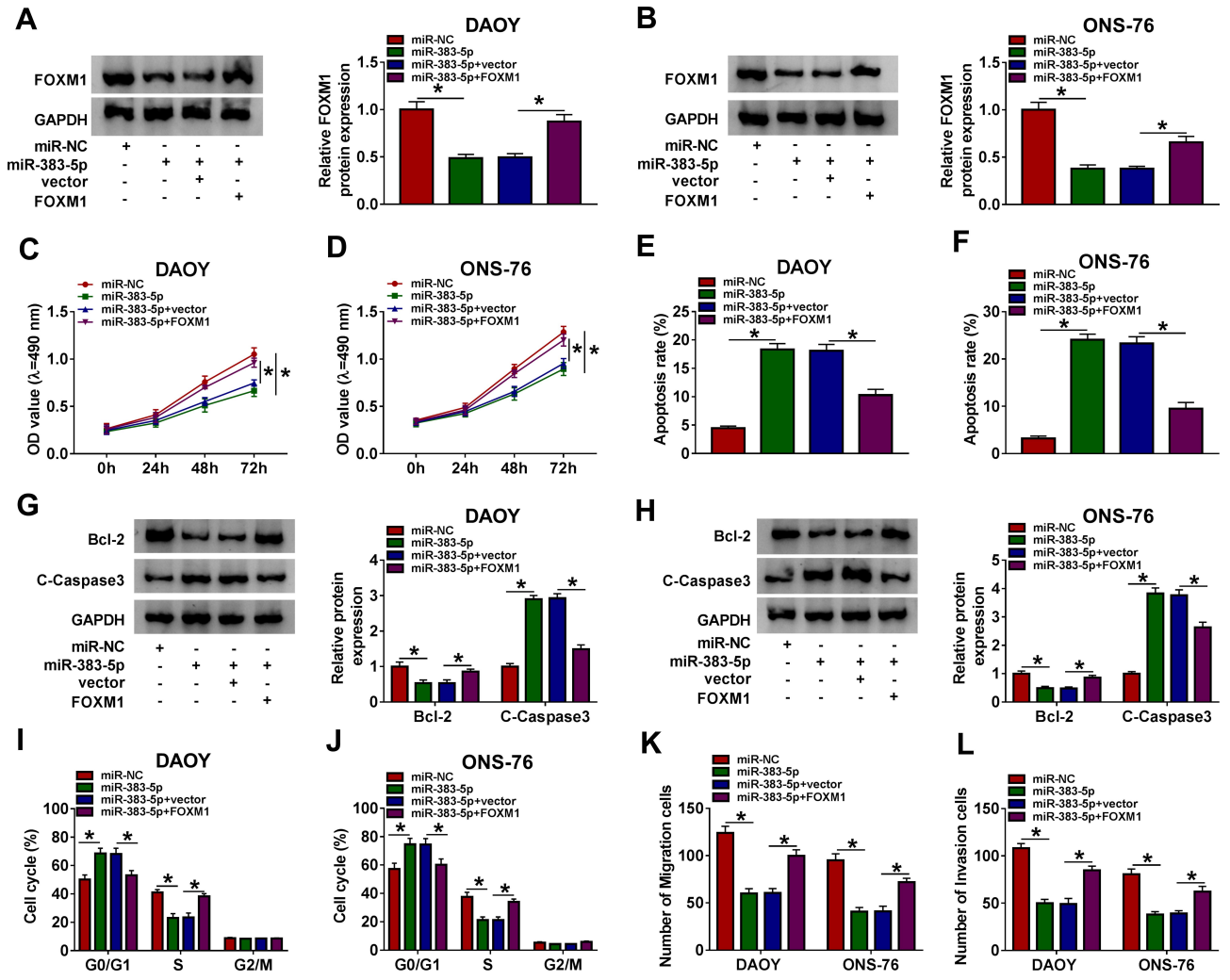

Figure 6 miR-383-5p confined cell proliferation, migration, and invasion while facilitated apoptosis in DAOY and ONS-76 cells by targeting *FOXM1*. (**A**–**J**) The DAOY and ONS-76 cells were transfected with miR-NC, miR-383-5p, miR-383-5p + vector, or miR-383-5p + FOXM1. (**A** and **B**) The protein level of FOXM1 was examined by Western blot. (**C** and **D**) The cell viability was monitored via MTT assay. (**E** and **F**) The apoptosis rate was measured through flow cytometry. (**G** and **H**) The protein levels of Bcl-2 and C-Caspase3 were detected by Western blot assay. (**I** and **J**) Cell cycle progression was determined by flow cytometry. (**K** and **L**) The migration and invasion abilities were evaluated by Transwell assay. Error bar, SD; n=3 biological replicates. **P*<0.05.

β1.[18] A recent study indicated that circSKA3 was involved in the progression of MB.[17] In the current study, we found that circSKA3 was notably enhanced in MB. Furthermore, the silencing of circSKA3 curbed cell proliferation, metastasis but induced apoptosis. Besides, circSKA3 depletion restrained xenograft tumor growth in vivo. These data revealed that circSKA3 accelerated MB progression.

Convincing evidence elucidated that miR-383-5p was involved in tumor progression in many types of cancers. For instance, a study in ovarian cancer indicated that miR-383-5p was reduced in ovarian cancer, and its overexpression regulated cell behaviors and chemo-sensitivity by targeting *TRIM27*.[32] Another study demonstrated that miR-383-5p was down-regulated in gastric cancer, and overexpression of miR-383-5p impeded cell growth and metastasis.[33] In our research, miR-383-5p was down-regulated in MB tissues, and it was predicted as a target of circSKA3. The expression of miR-383-5p was suppressed by circSKA3 depletion. Besides, miR-383-5p inhibitor partly reversed the inhibition effects on cell viability, cell cycle progression, migration and invasion, as well as the promotion effect on cell apoptosis induced by si-circSKA3. These results unraveled that circSKA3 facilitated MB progression by suppressing miR-383-5p.

FOXM1 was related to tumor progression in diverse cancers. Wang et al implied that *FOXM1* was enhanced in human non-small cell lung cancer, and its overexpression boosted cell growth and metastasis in vitro.[34] Another

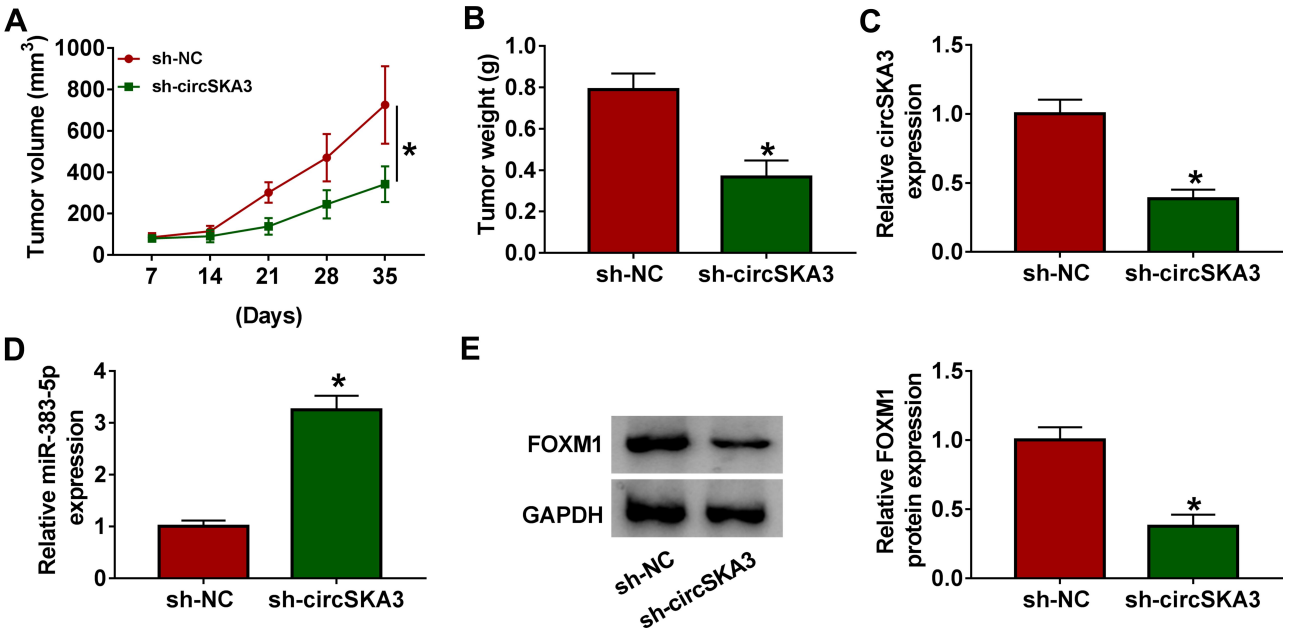

Figure 7 CircSKA3 silencing confined xenograft tumor growth in vivo. (**A**–**E**) The six-week-old male nude mice (n=6 per group) were injected subcutaneously into the right flank with DAOY cells stably transfected with sh-circSKA3 or sh-NC. (**A** and **B**) The volume and weight of xenograft tumor were exhibited. (**C** and **D**) The levels of circSKA3 and miR-383-5p were examined by qRT-PCR. (**E**) The protein level of FOXM1 was measured via Western blot assay. Error bar, SD; *P<0.05.

study in cervical cancer disclosed that the level of *FOXM1* was distinctly increased in cervical cancer, and its silencing blocked cell migration and invasion targeted by miR-214.[35] In the present research, *FOXM1* was obviously enhanced in MB and verified as a candidate of miR-383-5p. The expression of *FOXM1* in MB was in line with the results in the past document.[29,30] The promotion effect of miR-383-5p on cell apoptosis and the inhibition effect on cell proliferation, cell cycle progression, migration, and metastasis were reversed by *FOXM1*. Furthermore, circSKA3 silencing reduced *FOXM1* expression via miR-383-5p in MB. These results suggested that circSKA3 acted as a sponge of miR-383-5p, and then regulated *FOXM1* expression to accelerate MB progression.

In conclusion, these data suggested that circSKA3 depletion blocked MB progression by regulating *FOXM1* expression via miR-383-5p. This new regulatory pathway may shed light on the mechanism of MB and provide new markers for the early-stage diagnosis for MB patients.

Disclosure

The authors have no conflicts of interest to declare.

References

1. Northcott PA, Jones DT, Kool M, et al. Medulloblastomics: the end of the beginning. *Nat Rev Cancer*. 2012;12(12):818–834. doi:10.1038/nrc3410
2. Pui CH, Gajjar AJ, Kane JR, Qaddoumi IA, Pappo AS. Challenging issues in pediatric oncology. *Nat Rev Clin Oncol*. 2011;8(9):540–549. doi:10.1038/nrclinonc.2011.95
3. Gajjar AJ, Robinson GW. Medulloblastoma-translating discoveries from the bench to the bedside. *Nat Rev Clin Oncol*. 2014;11(12):714–722. doi:10.1038/nrclinonc.2014.181
4. Massimino M, Biassoni V, Gandola L, et al. Childhood medulloblastoma. *Crit Rev Oncol Hematol*. 2016;105:35–51. doi:10.1016/j.critrevonc.2016.05.012
5. Rutkowski S, von Hoff K, Emser A, et al. Survival and prognostic factors of early childhood medulloblastoma: an international meta-analysis. *J Clin Oncol*. 2010;28(33):4961–4968. doi:10.1200/jco.2010.30.2299
6. Gajjar A, Chintagumpala M, Ashley D, et al. Risk-adapted craniospinal radiotherapy followed by high-dose chemotherapy and stem-cell rescue in children with newly diagnosed medulloblastoma (St Jude Medulloblastoma-96): long-term results from a prospective, multicentre trial. *Lancet Oncol*. 2006;7(10):813–820. doi:10.1016/s1470-2045(06)70867-1
7. Spiegler BJ, Bouffet E, Greenberg ML, Rutka JT, Mabbott DJ. Change in neurocognitive functioning after treatment with cranial radiation in childhood. *J Clin Oncol*. 2004;22(4):706–713. doi:10.1200/jco.2004.05.186
8. Mabbott DJ, Spiegler BJ, Greenberg ML, Rutka JT, Hyder DJ, Bouffet E. Serial evaluation of academic and behavioral outcome after treatment with cranial radiation in childhood. *J Clin Oncol*. 2005;23(10):2256–2263. doi:10.1200/jco.2005.01.158
9. Ling H, Vincent K, Pichler M, et al. Junk DNA and the long non-coding RNA twist in cancer genetics. *Oncogene*. 2015;34(39):5003–5011. doi:10.1038/onc.2014.456
10. Huang T, Alvarez A, Hu B, Cheng SY. Noncoding RNAs in cancer and cancer stem cells. *Chin J Cancer*. 2013;32(11):582–593. doi:10.5732/cjc.013.10170
11. De Windt LJ, Giacca M. Non-coding RNA function in stem cells and regenerative medicine. *Noncoding RNA Res*. 2018;3(2):39–41. doi:10.1016/j.ncrna.2018.04.004

12. Anastasiadou E, Jacob LS, Slack FJ. Non-coding RNA networks in cancer. *Nat Rev Cancer*. 2018;18(1):5–18. doi:10.1038/nrc.2017.99
13. Zhang XO, Wang HB, Zhang Y, Lu X, Chen LL, Yang L. Complementary sequence-mediated exon circularization. *Cell*. 2014;159(1):134–147. doi:10.1016/j.cell.2014.09.001
14. Memczak S, Papavasileiou P, Peters O, Rajewsky N. Identification and characterization of circular RNAs as a new class of putative biomarkers in human blood. *PLoS One*. 2015;10(10):e0141214. doi:10.1371/journal.pone.0141214
15. Su H, Tao T, Yang Z, et al. Circular RNA cTFRC acts as the sponge of MicroRNA-107 to promote bladder carcinoma progression. *Mol Cancer*. 2019;18(1):27. doi:10.1186/s12943-019-0951-0
16. Bachmayr-Heyda A, Reiner AT, Auer K, et al. Correlation of circular RNA abundance with proliferation–exemplified with colorectal and ovarian cancer, idiopathic lung fibrosis, and normal human tissues. *Sci Rep*. 2015;5:8057. doi:10.1038/srep08057
17. Lv T, Miao YF, Jin K, et al. Dysregulated circular RNAs in medulloblastoma regulate proliferation and growth of tumor cells via host genes. *Cancer Med*. 2018;7(12):6147–6157. doi:10.1002/cam4.1613
18. Du WW, Yang W, Li X, et al. The circular RNA circSKA3 binds integrin β1 to induce invadopodium formation enhancing breast cancer invasion. *Mol Ther*. 2020;28(5):1287–1298. doi:10.1016/j.ymthe.2020.03.002
19. Memczak S, Jens M, Elefsinioti A, et al. Circular RNAs are a large class of animal RNAs with regulatory potency. *Nature*. 2013;495(7441):333–338. doi:10.1038/nature11928
20. Garzon R, Calin GA, Croce CM. MicroRNAs in cancer. *Annu Rev Med*. 2009;60:167–179. doi:10.1146/annurev.med.59.053006.104707
21. Singh SV, Dakhole AN, Deogharkar A, et al. Restoration of miR-30a expression inhibits growth, tumorigenicity of medulloblastoma cells accompanied by autophagy inhibition. *Biochem Biophys Res Commun*. 2017;491(4):946–952. doi:10.1016/j.bbrc.2017.07.140
22. Panwalkar P, Moiyadi A, Goel A, et al. MiR-206, a cerebellum enriched miRNA is downregulated in all medulloblastoma subgroups and its overexpression is necessary for growth inhibition of medulloblastoma cells. *J Mol Neurosci*. 2015;56(3):673–680. doi:10.1007/s12031-015-0548-z
23. Jiang J, Xie C, Liu Y, Shi Q, Chen Y. Up-regulation of miR-383-5p suppresses proliferation and enhances chemosensitivity in ovarian cancer cells by targeting TRIM27. *Biomed Pharmacother*. 2019;109:595–601. doi:10.1016/j.biopha.2018.10.148
24. Hu Y, Ma Y, Liu J, Cai Y, Zhang M, Fang X. LINC01128 expedites cervical cancer progression by regulating miR-383-5p/SFN axis. *BMC Cancer*. 2019;19(1):1157. doi:10.1186/s12885-019-6326-5
25. Xu G, Li N, Zhang Y, Zhang J, Xu R, Wu Y. MicroRNA-383-5p inhibits the progression of gastric carcinoma via targeting HDAC9 expression. *Braz J Med Biol Res*. 2019;52(8):e8341. doi:10.1590/1414-431x20198341
26. Kalinichenko VV, Major ML, Wang X, et al. Foxm1b transcription factor is essential for development of hepatocellular carcinomas and is negatively regulated by the p19ARF tumor suppressor. *Genes Dev*. 2004;18(7):830–850. doi:10.1101/gad.1200704
27. Yang SS, Gao Y, Wang DY, et al. Overexpression of eukaryotic initiation factor 5A2 (EIF5A2) is associated with cancer progression and poor prognosis in patients with early-stage cervical cancer. *Histopathology*. 2016;69(2):276–287. doi:10.1111/his.12933
28. Wang X, Jin Y, Zhang H, Huang X, Zhang Y, Zhu J. MicroRNA-599 inhibits metastasis and epithelial-mesenchymal transition via targeting EIF5A2 in gastric cancer. *Biomed Pharmacother*. 2018;97:473–480. doi:10.1016/j.biopha.2017.10.069
29. Priller M, Pöschl J, Abrão L, et al. Expression of FoxM1 is required for the proliferation of medulloblastoma cells and indicates worse survival of patients. *Clin Cancer Res*. 2011;17(21):6791–6801. doi:10.1158/1078-0432.ccr-11-1214
30. Zang W, Wang T, Wang Y, et al. Knockdown of long non-coding RNA TP73-AS1 inhibits cell proliferation and induces apoptosis in esophageal squamous cell carcinoma. *Oncotarget*. 2016;7(15):19960–19974. doi:10.18632/oncotarget.6963
31. Zhou R, Wu Y, Wang W, et al. Circular RNAs (circRNAs) in cancer. *Cancer Lett*. 2018;425:134–142. doi:10.1016/j.canlet.2018.03.035
32. Shen PF, Chen XQ, Liao YC, et al. MicroRNA-494-3p targets CXCR4 to suppress the proliferation, invasion, and migration of prostate cancer. *Prostate*. 2014;74(7):756–767. doi:10.1002/pros.22795
33. Li XT, Wang HZ, Wu ZW, et al. miR-494-3p regulates cellular proliferation, invasion, migration, and apoptosis by PTEN/AKT signaling in human glioblastoma cells. *Cell Mol Neurobiol*. 2015;35(5):679–687. doi:10.1007/s10571-015-0163-0
34. Wang X, Chen D, Gao J, et al. Centromere protein U expression promotes non-small-cell lung cancer cell proliferation through FOXM1 and predicts poor survival. *Cancer Manag Res*. 2018;10:6971–6984. doi:10.2147/cmar.s182852
35. Hong H, Zhu H, Zhao S, et al. The novel circCLK3/miR-320a/FoxM1 axis promotes cervical cancer progression. *Cell Death Dis*. 2019;10(12):950. doi:10.1038/s41419-019-2183-z